Monitoring the Daily Evolution and Extent of Snow Drought

Benjamin J. Hatchett[1], Alan M. Rhoades[2], and Daniel J. McEvoy[1]

[1]Desert Research Institute, Reno, Nevada, USA, 89512
[2]Climate and Ecosystem Sciences Division, Lawrence Berkeley National Laboratory, Berkeley, California, USA, 94720

Correspondence: Benjamin J. Hatchett (benjamin.hatchett@gmail.com)

Abstract. Snow droughts are commonly defined as below average snowpack at a point in time, typically 1 April in the western United States (wUS). This definition is valuable for interpreting the state of the snowpack but obscures the temporal evolution of snow drought. Borrowing from dynamical systems theory, we applied phase diagrams to visually examine the daily evolution of snow water equivalent (SWE) and accumulated precipitation conditions in maritime, intermountain, and continental snow climates in the wUS using station observations as well as spatially distributed estimates of SWE and precipitation. Using a percentile-based drought definition, phase diagrams of daily observed SWE and precipitation highlighted decision-relevant aspects of snow drought such as onset, evolution, and termination. The phase diagram approach can be used in tandem with spatially distributed estimates of daily SWE and precipitation to reveal variability in snow drought type and extent. When combined with streamflow or other environmental data, phase diagrams and spatial estimates of snow drought conditions can help inform drought monitoring and early warning systems and help link snow drought type and evolution to impacts on ecosystems, water resources, and recreation. A web tool is introduced allowing users to create real-time or historic snow drought phase diagrams.

1 Introduction

Snow-dominated mountains provide critical water resources to ecosystems and society (???), but their snowpacks are susceptible to climate warming (????). Warming impacts mountain regions in many ways, including reductions in the amount of water stored in snowpack (?), earlier spring snowmelt (??), and slower snowmelt (?). Warming increases will increase the frequency of extreme rain-on-snow events (?) and generally decreases the fraction of precipitation falling as snow (?). As rain falls instead of snow, runoff becomes could become less efficient (?) , a process amplified by increasing atmospheric demand for moisture (?). as water is no longer stored in the snowpack and as warming increases atmospheric water demand (?). However, seasonal shifts in energy availability altering plant available water storage (?) may counteract reduced snowmelt rates and changes in rain and snow partitioning, potentially buffering runoff changes in energy-limited (colder) environments.

Spring snowpack is Despite challenges in constraining mountain hydrologic sensitivity to warming, spring snowpack remains an important predictor of warm season runoff for environmental flows and human consumptive use . Projected snowpack losses in upwards of 89% of areas in many regions ?. Peak snow water equivalent is projected to decline by 40-60% in the western United States (wUS) by end-century ?. For regions historically characterized by a seasonal snowpack by end-century , these declines will reduce drought prediction skill in these regions (?). (?). Losses will be pronounced in lower elevation coastal

1

snowpacks that are most "at risk" to warming (**????**). ~~In addition to downstream agricultural (**?**), environmental (**??**) and other economic impacts (**??**), reductions~~ Reductions in snowpack negatively impact wildlife habitat (**?**) and decrease opportunities for recreation and tourism (**???**) ~~. In many~~ in addition to downstream agricultural (**?**), environmental (**??**) and other economic impacts (**??**). In rural mountain regions, winter recreation and tourism ~~are~~ form pillars of the economy (**?**).

Tracking snowpack throughout the wUS cool season (~~defined broadly as November-May~~typically November-April) and identifying below-normal snow conditions known as "snow drought" (**????**) aids resource managers in making decisions (e.g., water allocations or the timing and magnitude of runoff) based on the state of the snowpack relative to past and forecast ~~conditions and forecast~~ weather and snowpack conditions. Often, a point-in-time approach is used to assess snowpack conditions pertaining to runoff. For example, the date of 1 April is codified into many wUS water management agencies (**?**) that depend on runoff from both seasonal and ephemeral snowpacks (**?**) to assess warm season water availability. The relation of this date to peak snowpack timing and its representatives of the total volume of potential meltwater, however, varies by location and season (**????**). **?** highlight other challenges of the single point-in-time definition. Notably, they discussed that pre-1 April snow droughts can be obscured by later heavy snowfall and that anomalous melt events during warmer-than-normal conditions can create snow drought conditions not directly related to precipitation. In addition, no clear definition for snow drought onset has been provided. **?** used 80% of average SWE, whereas **?** used below normal. Depending on snowpack accumulation, which varies by widely within and between regions, snow droughts may occur across a range of percentages of normal and are not easily comparable. This motivates the use of a percentile-based approach to facilitate regional comparisons.

These challenges, and the need to communicate mountain hydroclimate conditions to varied user groups (e.g., the National Weather Service, natural resource managers and other decision makers (**?**)), illustrate the need for easily-accessible, informative data visualization approaches~~that~~ . Ideally, these visualizations capture the signals of interest for decision-relevant contexts and ~~allows~~ allow a user to track ~~their~~ snowpack and precipitation evolution through the cool season or the entire water year (WY). Here ~~,~~ we introduce the application of phase diagrams ~~which enable the visualization of~~ that enable visualizing how two variables co-vary through time. Specifically, we show the daily temporal co-evolution of snow water equivalent (SWE) and precipitation. We ~~also~~ demonstrate the utility of this approach using examples across a range of spatial scales in wUS snow-dominated regions. We also highlight intraseasonal and interannual snowpack variability, snow drought variation along an elevational and longitudinal transect, and how dry snow droughts (below-average precipitation and snowpack) versus warm snow droughts (above-average precipitation but below-average snowpack) differ. Last, a web-based tool enabling the creation of phase diagrams "in real time" based on the SNOTEL network is introduced: https://wrcc.dri.edu/my/climate/snow-drought-tracker.

2 Data

2.1 Station Observations

Daily observations of SWE and accumulated WY precipitation (the WY begins on 1 October and ends on 30 September, with the year corresponding to the latter date) were acquired from seven SNOwpack TELemetry (SNOTEL) stations from the Natural Resources Conservation Survey (https://www.wcc.nrcs.usda.gov/snow/) across the wUS (Figure 1; Table 1). SNOTEL

is a long-term, quality-controlled, surface-based network for observing precipitation and snow in wUS mountains (**?**). We used SNOTEL stations located in California, Colorado, Nevada, Utah, and Washington (Table 1). These stations ~~exemplify a range of~~ capture three primary snow climates (maritime, intermountain, and continental; (**?**)). We acquired daily SNOTEL data spanning the period of record (typically beginning in the 1980s) through 31 May ~~,~~ 2020 for complete WYs. We recommend only using stations with at least 20 years of data. In our example highlighting the web-based tool, we used an end date of 8 March ~~,~~ 2021 to show the real-time application of phase diagrams. Last, we highlight an example of how snow drought conditions influence streamflow and to show how to link phase diagrams with hydrologic outcomes. To do so, we acquired daily streamflow for WYs 1943–2019 from the U.S. Geological Survey Gage 12082500, located on the unimpaired Nisqually River, near the Paradise, Washington SNOTEL site (1b)~~to show how to link phase diagrams with hydrologic outcomes~~.
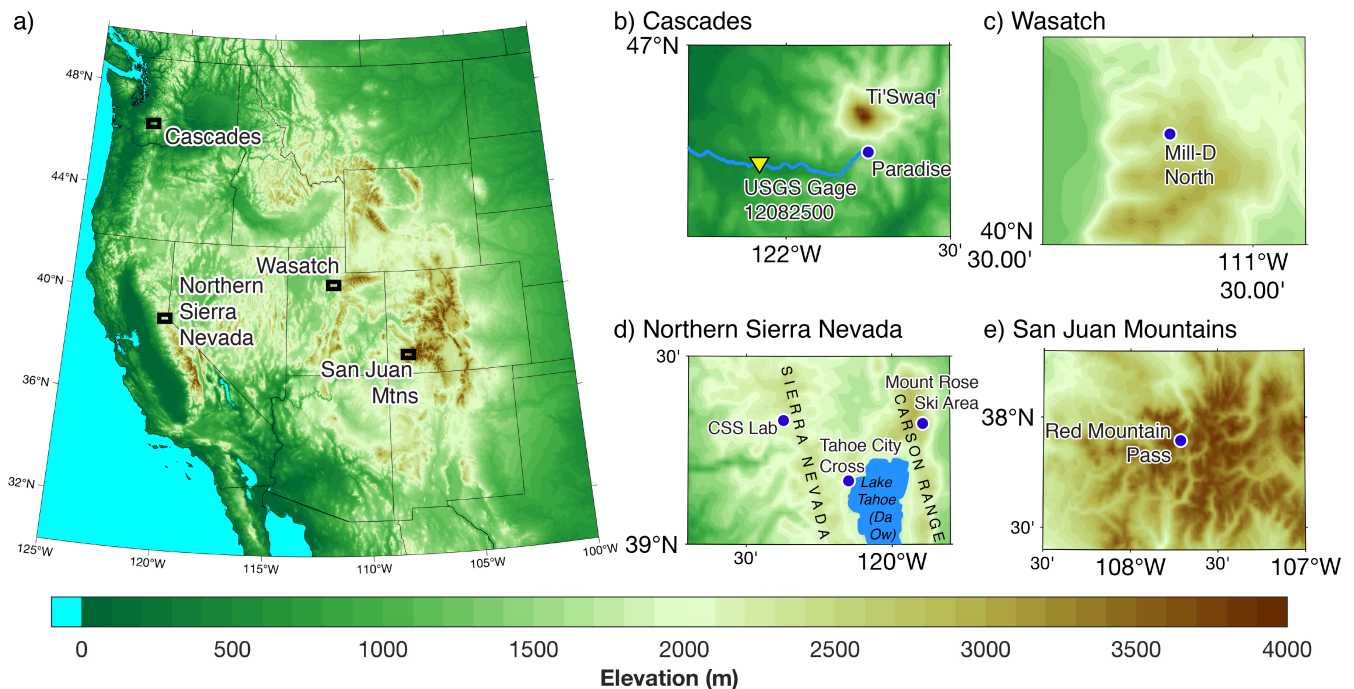

Figure 1. (a) Digital elevation map of western United States topography (in m) from ETOPO (**?**) showing focus study areas~~of focus~~: **(b)** the Cascade Mountains, **(c)** the Wasatch Mountains, **(d)** the Northern Sierra Nevada, and **(e)** the San Juan Mountains. SNOTEL stations are shown by blue dots. The yellow triangle indicates the U.S. Geological Survey Gage 12082500 on the Nisqually River.

2.2 Gridded Observational Products

To add a spatial component to station-based SWE and precipitation phase diagrams, we utilized daily gridded 4 km resolution estimates of SWE for the continental U.S. ~~, herein called~~ produced by the University of Arizona ~~SWE reanalysis ((~~hereafter UAswe; **??**). The UAswe product spans WYs 1982–2020. Daily, gridded 4 km spatial resolution precipitation was acquired

Table 1. Metadata for western United States SNOwpack TELemetry (SNOTEL) stations used to generate the phase diagrams.

Station Name	Elev. m)	Lat (°N)	Lon (°W)	Start Date	Snow Climate
CSS Lab, CA	2201	39.33	-120.37	Oct 1983	Maritime
Mill-D North, UT	2733	40.66	-111.64	Oct 1988	Intermountain
Mount Rose Ski Area, NV	2683	39.32	-119.89	Oct 1980	Intermountain
Paradise, WA	1564	46.78	-121.75	Oct 1980	Maritime
Red Mountain Pass, CO	3414	37.89	-107.71	Oct 1980	Continental
Tahoe City Cross, CA	2072	39.32	-120.15	Oct 1980	Maritime
Virginia Lakes, CA	2866	38.07	-119.23	Oct 1978	Intermountain

from gridMET (**?**). Phase diagrams can be applied to any long-term daily ~~in-situ~~ in-situ and/or gridded SWE product and ~~is~~ are not limited to the observational products chosen in this study. Examples of watershed-averaged phase diagrams are presented

75 and compared with nearby SNOTEL stations for two, eight digit U.S. Geological Survey Hydrologic Unit Codes (HUC-8) watersheds ~~?~~ (**?**) in the Sierra Nevada (The Upper Yuba River Basin and the Tuolumne River Basin).

3 Methods

3.1 Visualizing snow drought with a phase diagram

The concept of phase diagrams were initially developed by Ludwig Boltzmann, Henri Poincaré, and Josiah Willard Gibbs

80 (**?**). The intent was to represent all possible states of a dynamical system, such as a particle's position and momentum. Many disciplines now use phase diagrams (also referred to as phase space diagrams)—including nonlinear dynamics, chaos theory, as well as statistical and quantum mechanics. Each parameter of the system in phase diagrams ~~are~~ is represented by an axis of a multidimensional space. In a two-dimensional system, each point on the phase plane represents a combination of the system's parameters, with the evolution of the system's state through time tracing a line called the phase space trajectory. The phase

85 space trajectory begins at the point representing the initial conditions. Depending on the application, the trajectory continues indefinitely or until the time period of interest has elapsed.

Inspired by the simplicity of phase diagrams, specifically the Wheeler-Hendon phase diagrams used to track the phase and life cycle of the tropical intraseasonal Madden-Julian Oscillation (**?**), our purpose is to show how this visualization approach can track SWE and precipitation conditions during the cool season. We aim to track the phase space of cool season mountain

90 hydroclimate conditions in order to link them to the trajectory of snow drought conditions (dry and warm; (**?**)) to the hydrometeorological events (**?**) shaping the trajectories. Thus, phase diagrams can ~~be used to~~ help diagnose snow drought onset, termination, duration, type, and severity as well as explore timing and characteristics of large 'drought-busting~~storms'~~' storms (**?**). By implicitly including ~~these mixture effects~~ the time-varying effects of precipitation and temperature, phase diagrams provide a unique perspective over time series plots in tracking snowpack conditions. For instance, phase diagrams can ~~be used~~

95 ~~to more~~ clearly show the abrupt changes in one or both variables during major accumulation or melt events.

3.1.1 Creating the Snow Drought Phase Diagram

For each station, we calculated daily percentiles of accumulated precipitation and SWE from 1 November to 30 April (or 31 May) using a seven-day moving window centered on each calendar day . to reduce seasonality effects (??). Results were not sensitive to moving windows sized between zero and 15 days. We calculated percentiles using the period of record. Following
?, we used the U.S. Drought Monitor "D scale" (**?**) to characterize snow drought as abnormally dry (D0), moderate drought (D1), severe drought (D2), extreme drought (D3), and exceptional drought (D4) for values between the 30th-20th, 20th-10th, 10th-5th, 5th-2nd, and below the 2nd percentiles, respectively. Following the Drought Monitor scale, snow drought is defined as SWE percentiles less than or equal the 30th percentile, which is slightly more inclusive than **?** who selected the 25th percentile as their threshold. Accumulated precipitation percentiles were plotted on the x-axis and SWE percentile on the y-axis. Each daily point was coloured by the corresponding month and connected by a line to create the phase trajectory. Snow drought severity, following the D scale, were denoted by colored lines. We defined the start of snow drought phase diagrams at the beginning of the WY onset when snow accumulation typically occurs (1 OctoberNovember), however they could be started at any time deemed relevant (i.e., 1 October or 1 December). Each trajectory point is binned by a unique color for a given WY month and the first day of each month is indicated by an emboldened letter. We selected the Depending on location, we selected either 30 April or 31 May for the termination of trajectories, denoted by a gold star. By the end of Maythese times, most water-related decisions based upon snowpack have been made.

3.2 Analysis of Gridded Products

For each 4 km SWE grid cell, we calculated daily percentiles of median SWE from 1 October–31 May for WYs 1982–2020, again using a seven-day moving window. The same approach was performed for gridMET precipitation. Snow drought is defined similarly as above, when SWE is at or below the 30th percentile. Several boundary regions (e.g., HUC-8boundaries) were used to calculate basin averages (means) for the gridded products whose grid points fell on or within the HUC-8 boundary.

3.3 Cumulative Discharge Calculations

Cumulative discharge at the Nisqually River U.S. Geological Survey stream gage was calculated for all complete WYs starting on the first day (1 Oct). For each day until the end of the WY (30 Sept), the accumulated discharge was calculated. For each WY, we calculated the date when 50% of the WY total accumulated discharge occurred. Median dates of 50% of WY total discharge were calculated using the full period of record.

4 Results and Discussion

4.1 An Example Annotated Phase Diagram

WY2020 was characterized by notable snowpack and precipitation variability throughout the cool season in the northern Sierra Nevada (Figure 2a). Both fall and late winter featured near record-low precipitation and snowpack at the Central Sierra Snow

Laboratory (CSS Lab). The upper right quadrant represents wet and snowy "Big Year" conditions when both accumulated precipitation and SWE exceed the 50th percentile. The upper left indicates SWE was above the median but accumulated precipitation was below median. Trajectories into this "Dry But Snowy" quadrant can result from dry fall conditions followed by appreciable snowfall, especially in places that normally receive fall precipitation as rain, or in lower elevation, warmer

130   locations when anomalous snowfall has occurred instead of ~~mixed rain and snow events~~rainfall. A drying fall has been identified as one signal of climatic change in California (**?**) and elsewhere in the wUS (**?**). This drying could induce a systematic leftward shift in future phase diagram trajectories during the 21st century. ~~During the melt season, persistent cold and dry conditions can drive trajectories upwards into the first or second quadrants as snow melts slower than expected historically, as occurred during May 2020.~~ In addition, a shift in precipitation timing into the colder months of the season could also drive a leftward
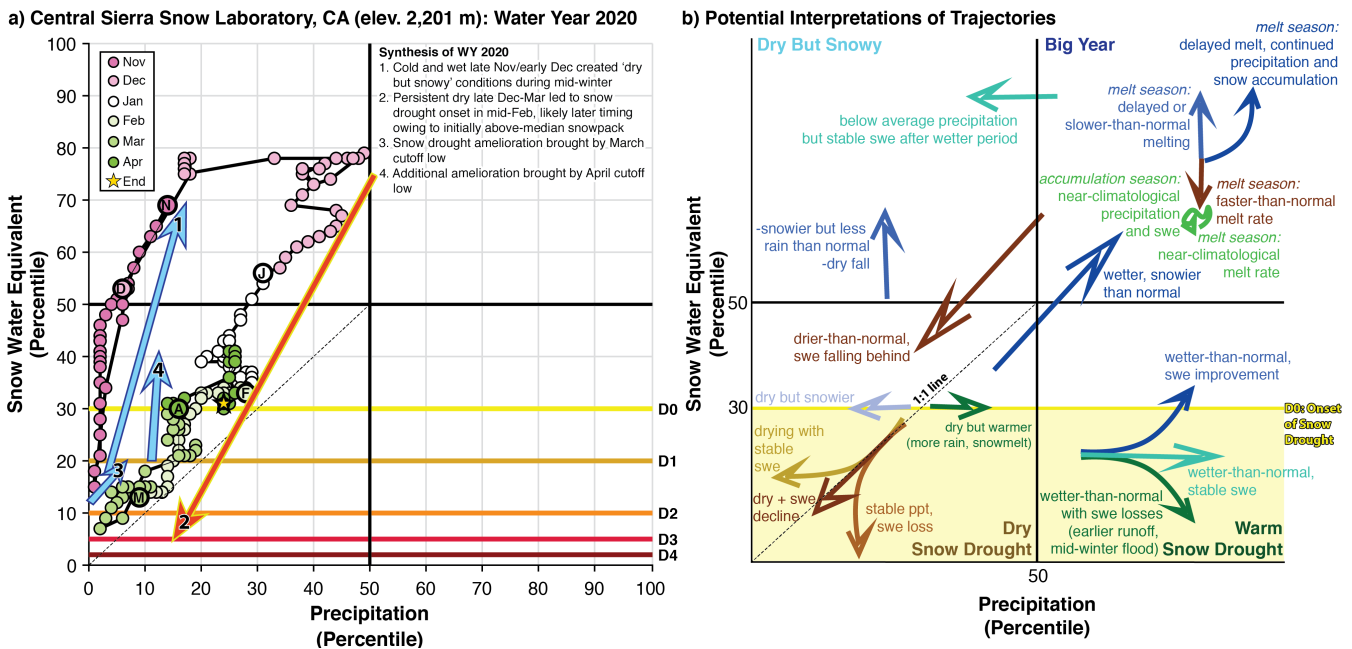
135   shift (**?**).

Figure 2. (a) Annotated phase diagram showing 1 ~~October,~~ November 2019 to ~~31 May,~~ 30 April 2020 at the Central Sierra Snow Laboratory (CSS Lab), California. ~~Percentiles are calculated based on period of record data.~~ **(b)** Conceptual phase diagram showing potential physical interpretations of seasonal evolution of various trajectories.

Dry snow drought conditions (meteorological drought) are identified in the lower left (third quadrant) when SWE falls into the D0-D4 range (i.e., less or equal to the 30th percentile) and accumulated precipitation is below the median. We defined warm snow drought when ~~satisfies snow drought conditions~~ SWE falls to below the 30th percentile and accumulated precipitation is greater than the median (lower right, or fourth quadrant). An additional case of 'dry-but-warm' snow drought occurs

140   when trajectories are in the dry quadrant but skew towards the wetter side of a 1:1 line (dashed line in the dry snow drought

quadrants). These conditions indicate drier-than-average conditions overall but with precipitation events that did not favor snowpack accumulation. To facilitate connecting various trajectories of phase diagrams with driving processes, the annotated figure is paired with a conceptual diagram showing potential physical interpretations (Figure 2b).

The start of WY2020 was characterized by bottom 3rd percentile precipitation conditions with low (bottom 20th percentile) snowpack at the CSS Lab (Figure 2a). Precipitation falling as snow led to rapid improvement from snow drought into the "Dry But Snowy" quadrant during late November into December, with precipitation recovering to ~~near-normal~~ near-median by mid-December. Persistent dry conditions lasting from late December through mid-March, driven by a blocking ridge west of North America (**?**), yielded snow drought onset in late January. Above-normal temperatures and dry conditions in late February and early March caused snowpack declines to accelerate, reaching a minimum value in the 5th percentile. Given that California receives the majority of its annual precipitation between December and March, dry spells ~~will quickly~~ lead to declines in precipitation percentile (trajectories move leftward; Figure 2a). WY2020, like other Sierra Nevada drought years, was notable for its lack of atmospheric river (AR) landfalls (**?**). ARs produce abrupt upwards and/or rightwards trajectories in the phase diagram via heavy precipitation (**?**) enhanced by orography (**?**). Snow drought amelioration in late March occurred when heavy snowfall resulted from a slow-moving cutoff low pressure system (**?**). By 1 April, the historically assumed peak timing of snowpack in the wUS (e.g., **?**), snow drought conditions remained but ~~had improved~~ SWE percentiles increased from the 5th to nearly the 30th percentile, though precipitation remained in the bottom 15th percentile. Another cutoff low in early April provided additional snow that terminated snow drought conditions, however accumulated precipitation remained below the median. This ~~further~~ highlights the importance of late spring (i.e., post-1 April) ~~meteorological~~ weather events in improving hydroclimatic conditions and a potential pitfall of assessing drought conditions at a single point in time. ~~The remainder of April and May were drier-than-normal, but snowmelt occurred slower than climatology, with above-median snowpack observed in mid-May.~~ By annotating the phase diagram, the story of the cool season can be expressed to show the key events producing observed outcomes (Figure 2b).

4.2 Snow Drought Variation in Time and Space

Weather events drive elevation-dependent changes in snowpack and snow drought conditions (**?**). In regions located near climatological expected rain-snow transition elevations (**?**), such as the Sierra Nevada, individual storms can produce dramatically different responses in snowpack spatial variability and magnitude. ARs are a common type of storm event yielding variable snowpack and hydrologic responses as a result of heavy precipitation with high ~~snow line~~ snowline elevations (**???**) or with ~~snow line~~ snowline elevations that vary widely over the duration of the storm (**??**).

WY2018 was emblematic of the aforementioned variation in rain and snow transition elevations as both elevation- and spatially-dependent responses to storms and dry spells occurred in the Sierra Nevada (Figure 3). WY2018 began with varying precipitation and SWE percentiles between three stations, again in the "Dry But Snowy" quadrant at the lower elevation stations (CSS Lab and Tahoe City Cross) and near climatology for the high elevation station (Mount Rose Ski Area). A late November AR event was followed by a multi-month dry spell that terminated in late February. Snowpack and precipitation

~~conditions improved~~ increased markedly in March, (colloquially termed a "Miracle March"), due to persistent stormy condi-
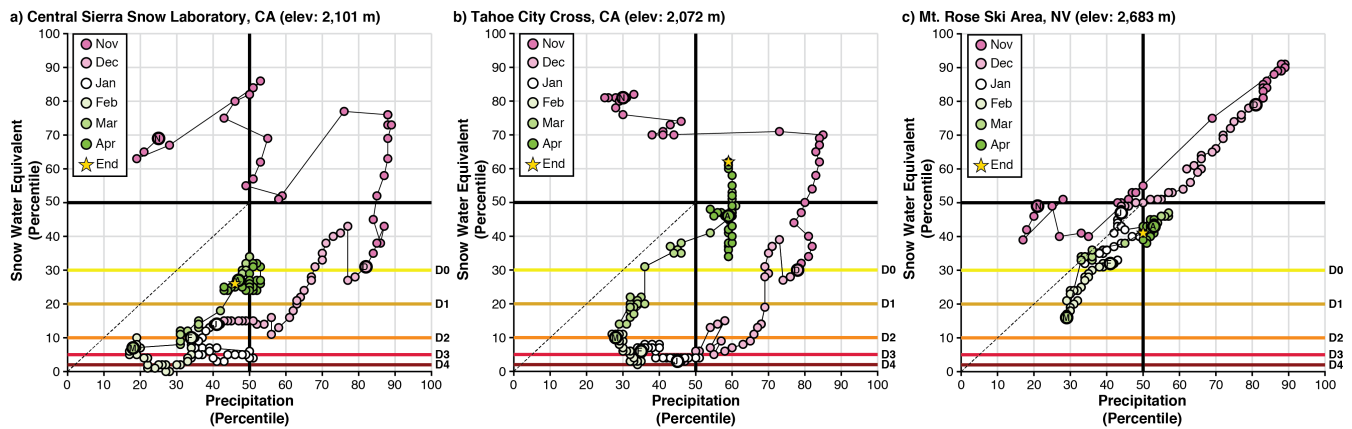tions associated with multiple landfalling ARs ~~and/or~~ associated with strong midlatitude cyclones.

Figure 3. An elevation-longitudinal examination of snow drought conditions during water year (WY) 2018 in the northern Sierra Nevada of California and Nevada. Stations are ordered from west to east: **(a)** CSS Lab, **(b)** Tahoe City Cross, and **(c)** Mount Rose Ski Area.

To highlight the elevation-induced heterogeneity of snowpack response within WY2018, we investigate three different stations situated along a similar longitude (Figure 1c). The late November warm and wet storm caused the CSS Lab and Tahoe City Cross (Figure 3a-b); both maritime snow climates) to shift rightwards and then downwards into the warm snow drought quadrant because much of the precipitation fell as rain. The CSS Lab is located along the Sierra Nevada crest while Tahoe City Cross is located further east in the rain shadow of the Sierra Nevada~~crest~~. Unlike the other two stations, the higher elevation Mount Rose Ski Area (hereafter "Mount Rose"), located further east in the Carson Range in a more intermountain snow climate (colder and drier than a maritime snow climate), received all snow. Mount Rose began the meteorological winter with 80th percentile precipitation and SWE ("Big Year"; Figure 3c). The CSS Lab and Tahoe City Cross received snow early in December, briefly moving each location out of warm snow drought. During the subsequent dry spell, the lower elevation CSS Lab and Tahoe City Cross stations both moved leftward from warm snow drought into dry snow drought, with a 30 percentile point decline in SWE through December. Dry snow drought conditions began at Mount Rose in early February. Importantly, the role of elevation is highlighted ($\sim$600 meter range between stations) with the colder Mount Rose experiencing less dramatic snowpack declines (reaching a minimum of the 16th percentile) compared to the warmer CSS Lab (minimum of 1st percentile) and Tahoe City Cross (minimum of 2nd percentile).

The return of North Pacific storminess during late February into March ~~brought notable improvement in~~ improved precipitation and snowpack conditions. This period also highlighted how snow drought amelioration is influenced by ~~snow climate type and~~ elevation. During this period, Mount Rose received all precipitation as snow. As a result, SWE ~~improved~~ increased by 30 percentile points (~~out of~~ terminating snow drought) while precipitation ~~improved~~ increased from the 26th percentile to 52nd percentile (Figure 3c). The ~~maritime CSS Lab improved~~ CSS Lab increased its SWE by 35 percentile points from the lowest

8

on record for the date in late February to non-snow drought conditions by late March. Precipitation also ~~improved~~ increased by approximately 35 percentile points ~~, back~~ to near median values. The cold March storms demonstrated a weaker rain shadow and generally lower ~~snow levels. This improved~~ snowline elevations. This increased SWE at the Tahoe City Cross from the 2nd percentile to above the 40th percentile while precipitation also ~~improved~~ increased from the 26th to the 60th percentile between late February and early April (Figure 3b). ~~As a result of~~ Owing to "Miracle March", 1 April 2018 SWE conditions were closer to median than reflected by the majority of the winter, similar to WY2020 (Figure 2a). The record to near-record low, late winter SWE at the lower elevation CSS Lab and Tahoe City Cross are thus hidden by a single point-in-time perspective. WY2018 and WY2020 demonstrate the importance of a complete WY perspective regarding the assessment of evolving snow drought conditions, namely the importance of a few large precipitation events.

4.3 Warm Versus Dry Snow Drought: Implications for Runoff Timing

The warming-induced shift in precipitation phase from snow to rain has been shown in historical trends in the wUS (**?**) and is projected to continue in a warmer world (**???**). Precipitation phase transition from snow to rain will result in more frequent warm snow droughts (**??**). This increase will disproportionately impact climatologically warmer maritime snow climates (**?**) with important implications on the headwater hydrology and downstream reservoir management strategies of these watersheds ~~(??????)~~(?????). To provide a comparison of WYs that experience comparable snow drought conditions ~~(with respect to snowpack percentiles)~~, but differing drivers, we compared the WY2001 dry snow drought (Figure 4a) to the WY2015 warm snow drought (Figure 4b) at Paradise, Washington. Paradise is located in the Pacific Northwest on the south flank of Ti'Swaq' (Mount Rainier; Figure 1b). The WY2015 warm snow drought in the Pacific Northwest was a motivating and formative WY for the development of ~~modern~~ snow drought research (**?**).

Paradise spent the majority of the cool season of WY2001 in the bottom 10th precipitation percentile, a substantial difference from WY2015 when precipitation was between the 60th and 88th percentile between December and April. The warm snow drought resulted from an anomalous amount of precipitation largely falling as rain in the early portion of winter. Snowpack conditions marginally ~~improved~~ increased throughout WY2001 from below the 10th percentile in February to the 20th percentile by the end of the cool season (Figure 1a). However in WY2015, Paradise maintained fairly consistent SWE percentiles below the 10th percentile from February to May. The leftward trajectory of precipitation during February 2015 is indicative of drier-than-normal conditions followed by generally dry conditions (Figure 1b). Weak snow drought amelioration occurred in 2001, minimizing its water resource impacts, whereas none occurred in 2015, further highlighting the importance of monitoring snow drought conditions, and type, over an entire WY.

Figure 4(a-b) shows the entire WY phase diagrams and a SWE spatial extent snapshot at various times (d-k), relative to median climatology, for WY2001 and WY2015. We also highlight the differences in hydrologic outcomes between these dry and warm snow drought years (Figure 4c). WY2001 had the second lowest cumulative flows for the Nisqually River in the period studied (WY1943–2019), but 50% of the cumulative WY2001 flow occurred 30 days *later* than the median date (3 April) at which half the Nisqually flow occurs. In contrast, WY2015 demonstrated middle-of-the-range total WY flow (48th of 77 years) but achieved 50% of the WY flow 56 days *earlier* than average. This indicates a key difference between the WYs.
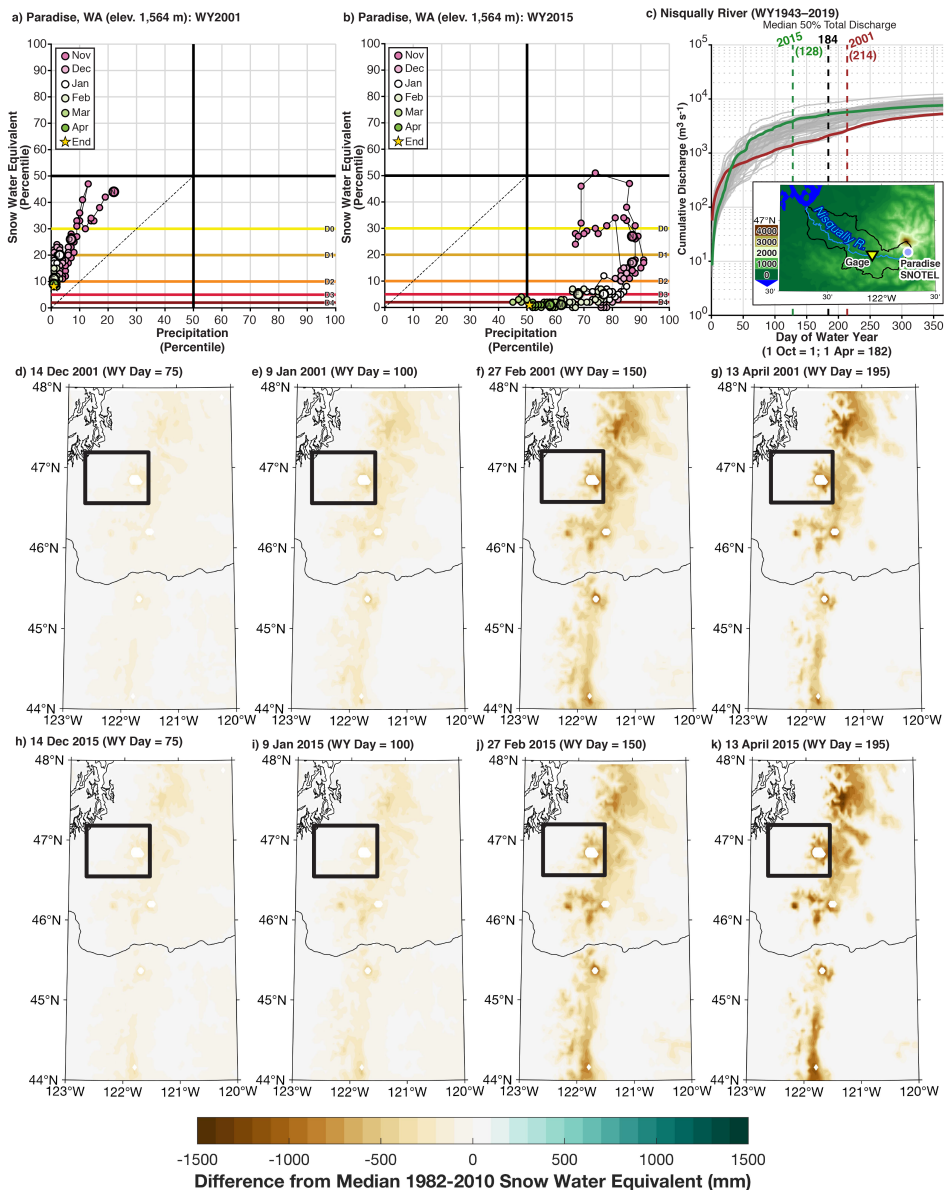
Figure 4. Comparison of dry **(a)** and warm **(b)** snow drought conditions in the Pacific Northwest at Paradise, Washington during water years (WY) 2001 and 2015, respectively. **(c)** Cumulative discharge (in $m^3 s^{-1}$) from the Nisqually River with vertical dashed lines indicating the date at which 50% of the total WY runoff occurred. **(d–g)** Spatial snow water equivalent anomalies (in mm) during WY2001 from the UAswe product (**?**). **(h–k)** As in **(d–g)** but for WY2015.

WY2015 had less snow water stored later into the season ~~, which markedly influenced~~ <u>than WY2001, markedly influencing</u>

230   <u>summer</u> streamflow. During both seasons, despite the vastly different precipitation regimes, spatial SWE anomalies are not

10

markedly different during mid-December (Figures 4d and 4h), mid-January (Figures 4e and 4i), or late February (Figures 4f and 4j). Consistent with lower SWE percentiles at Paradise during WY2015 compared to WY2001, as shown on the phase diagrams, SWE anomalies are modestly more negative. The lack of mountain snowpack during WY2015 was more notable than WY2001 (Figures 3g and 4k). The comparatively better spring snowpack in WY2001 likely helped maintain flows later into the year despite an otherwise dry year.

4.4 Interannual Variability

Enhanced interannual precipitation variability and decreased peak SWE variability are expectations of a warming climate (**???**). Comparisons of extreme years and their outcomes providing valuable object lessons for water managers and other resource planners (**??**). Phase diagrams allow for direct comparisons between WYs, helping to identify key differences in hydroclimate variability for a particular region of interest. ~~As a proof of concept~~For example, Red Mountain Pass, located in a high elevation, continental snow climate within the San Juan Mountains of southwestern Colorado, is used to compare two late cool season outcomes that represent two hydroclimatic extremes. The majority of WY2011 showed phase trajectories in the 'Big Year' first quadrant (Figure 5a) after a slightly below-average start to snowpack totals between October and early December. ~~An active~~ A stormy December increased SWE and precipitation percentiles. ~~Active~~ Stormy weather continued in April and May, preventing snowmelt and causing precipitation and SWE percentiles to increase. WY2012 began with above-average precipitation and snowpack in fall but drier-than-normal conditions throughout winter which resulted in dry snow drought onset in December (Figure 5b). Modest snow drought amelioration occurred in early March, but with a few exceptions in April, dry conditions persisted through May. This led to the onset of dry snow drought, again, via rapid snowmelt and below-average precipitation.

Spatial SWE distributions are consistent with the phase diagrams (Figure 5c-j). In both years, SWE anomalies increased throughout the accumulation season and then accelerated in late spring. Compared to the emerging drought signal during WY2012, WY2011 did not demonstrate widespread positive SWE anomalies throughout the year. Between January and April, lower elevation regions experienced below-normal SWE anomalies (Figure 5c-d), whereas higher elevations had above-normal SWE. This difference resulted from above-normal temperatures and below-normal precipitation, likely driven by snow-albedo feedbacks that were enhanced at lower elevations where snowmelt occurred (**??**).

4.5 ~~Basin-Averaged~~ Towards Visualizing the Type and Extent of Snow Drought ~~Phase Diagrams~~Across Space

We applied SNOTEL station data to create the phase diagrams, but a challenge in mountain environments is the lack of reliable, well-distributed, long-term observations. In lieu of station data, gridded observational products commonly inform natural resource decision-making and research efforts. The necessary components exist to create phase diagrams using gridded meteorological products (**??**), observation-based snow datasets (**??**), and output from hydrological simulations (**?**). The challenge is how to aggregate spatial information to extract maximum information value for the application of interest (e.g., water management, avalanche forecasting, ecosystem processes) regarding the state and evolution of snowpack conditions at relevant scales (e.g., the full watershed, a sub-basin, or within specific elevation bands) in complex terrain. We have performed a first step towards this goal. Initial methods to broaden the approach could be performed by: (1) binning regions by similar
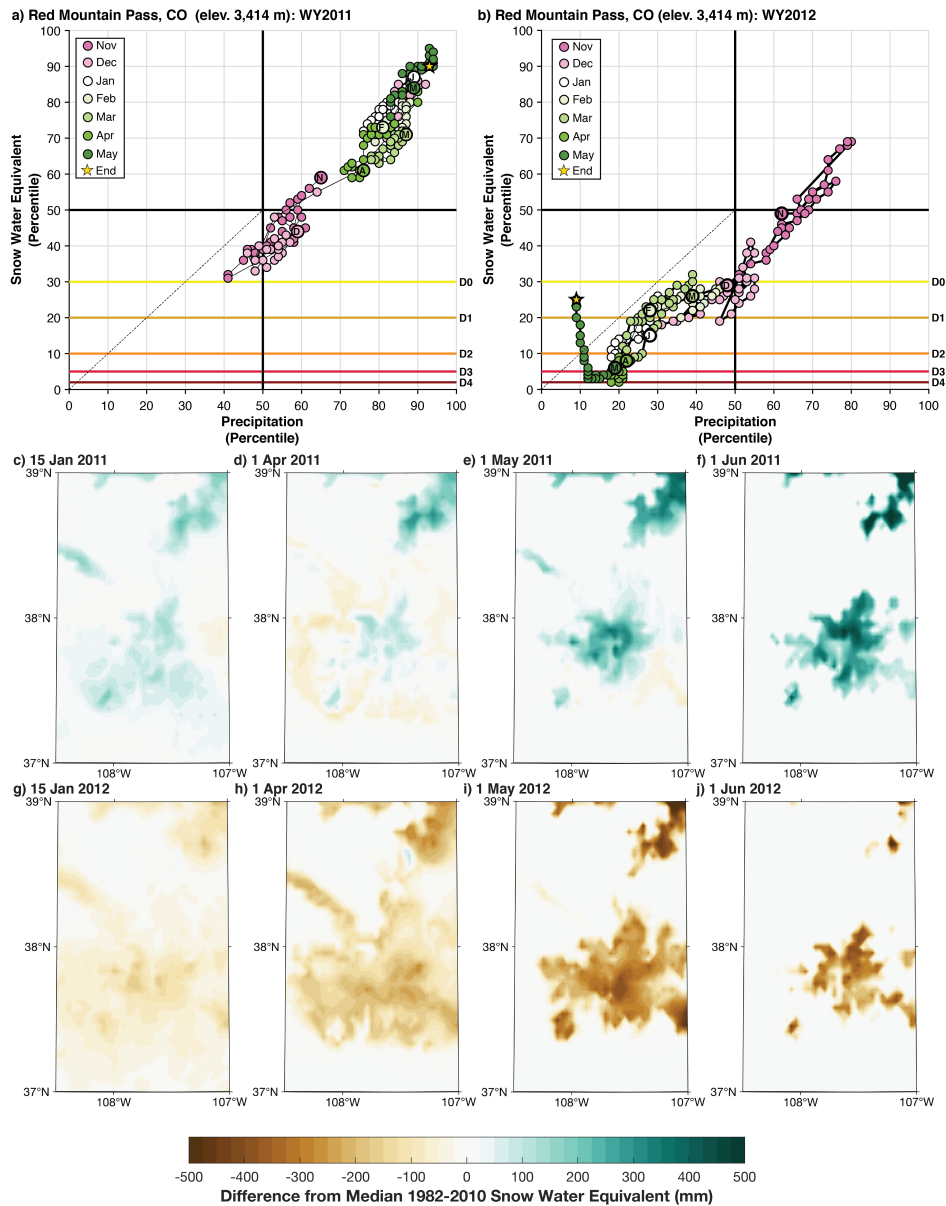
Figure 5. Comparison of an anomalously snowy and wet "big year" **(a)** and anomalously dry year **(b)** in the San Juan Mountains at Red Mountain, Colorado during water years (WY) 2011 and 2012, respectively. **(c-f)** Spatial snow water equivalent anomalies (in mm) during WY2011 for midwinter, early, middle, and late spring from the UAswe product (**?**). **(g-j)** As in **(c-f)** but for WY2012.

elevation, watershed, slope, aspect, and/or land cover type; (2) identifying areas that co-vary together in time and space using techniques such as principal component or cluster analysis; and (3) subjective grouping based on anecdotal information from

12

managers. Creating meaningful phase diagrams for varied management and scientific applications using spatially distributed information is the primary goal of our ongoing research. This will allow evaluation of snow drought in regions without long-term snow-observing networks such as in the northeastern U.S. or other high mountain areas worldwide. Towards this end, we next provide examples of how spatially distributed products can visualize snow drought.

4.5.1 Basin-Averaged Snow Drought Phase Diagrams

Aggregating spatially distributed information to the HUC-8 scale allows the creation of phase diagrams where few or no *in situ* observations exist. If such observations do exist, watershed-aggregated phase diagrams can be compared against station data, as shown in Figure 6 for WY2020 (see Section 4.1). We examine two Sierra Nevada watersheds, the relatively low elevation Upper Yuba River Basin and the relatively high elevation Tuolumne River Basin. Both have nearby SNOTEL stations, the CSS Lab station sits at the headwaters of the Yuba River while the Virginia Lakes station is located on the lee of the Sierra Nevada crest northeast of the Tuolumne River Basin.

In both cases, similarities exist between the SNOTEL and watershed-aggregated phase diagrams (Figure 6). The SNOTEL stations, which are located at higher elevations in the watershed, show wetter (above median) and snowier (above median) early season conditions during October and November (Figure 6a,c) whereas the watersheds show below median SWE and precipitation (Figure 6b,d). Late November and December brought substantial SWE improvement, with the Upper Yuba Basin moving into the "Dry But Snowy" quadrant (Figure 6b) and the Tuolumne River Basin extending further rightwards into the "Big Year" quadrant (Figure 6d). Virginia Lakes also ~~improved~~ increased into the "Dry But Snowy" quadrant (Figure 6c). Both regions followed similar trajectories downwards and to the left (SWE and precipitation falling behind; (Figure 2b)) during the extremely dry period spanning late December into mid-March and then underwent modest SWE recoveries with the ~~active~~ stormy spring ("Miracle March").

By the end of the cool season (~~31 May), the higher elevation Tuolumne River Basin experienced wetter conditions (22nd percentile)compared to the Upper Yuba Basin (5th percentile precipitation)~~ 30 April), both regions showed similar SWE percentiles (within 10 points). Precipitation percentiles were different by only a few points in the Tuolumne but by over 20 points in the Upper Yuba. These differences, as well as ~~exiting D0 snow drought (SWE > 30th percentile precipitation) while the Upper Yuba Basin remained in D2 (22th percentile SWE). This may reflect orographically enhanced precipitation and/or higher snowline elevation during the spring storms. The~~ the differences in trajectories throughout the winter, likely reflect the signal of orographically enhanced precipitation-or rain shadowing in the case of Virginia Lakes, which lies on the leeside of the Sierra Nevada crest. The CSS Lab was substantially wetter compared to the Upper Yuba during March and April of WY2020, whereas Virginia Lakes showed a similar trajectory but slightly shifted towards drier percentiles. The SNOTEL stations, likely by virtue of their location ~~at higher elevation, demonstrated opposite melt-out signals to the basin-aggregated phase diagrams. The SNOTELs increased in SWE percentile through May while the basin-wide percentiles declined. This result may stem from the~~ compared to the watershed hypsometry, may report higher SWE percentiles compared to the basin average if the SNOTEL station is located at a high elevation (CSS Lab) or lower SWE percentiles if the station is found at a middle elevation on the leeward (dry) side (Virginia Lakes).
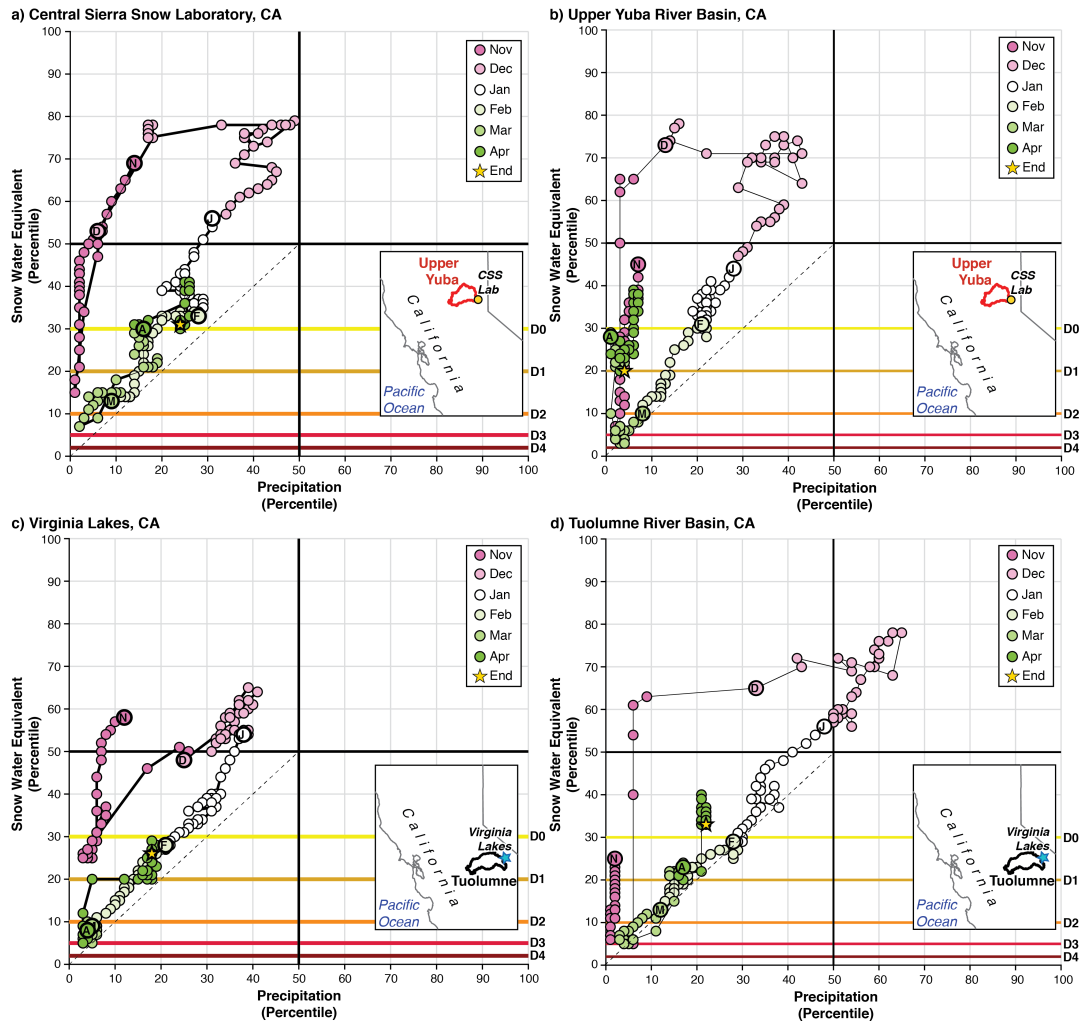
Figure 6. Phase diagrams for water year 2020: (**a**) CSS Lab SNOTEL, (**b**) Upper Yuba River Basin HUC-8, (**c**) Virginia Lakes SNOTEL, and (**d**) Tuolumne River Basin HUC-8. Locations of watersheds and SNOTEL stations are noted on inset maps.

300   The effects of topograhy could be exacerbated at the basin scale by the inclusion of lower elevation terrain ~~in the basin aggregations~~ whose snow rapidly melts out during drought years (potentially accelerated by snow-albedo feedbacks, e.g., **?**). While SNOTEL stations are placed with the intention of being representative for water resources given siting restrictions, the limitations created by varying topography and snowpack accumulation patterns warrants care in extrapolating data from a station to a basin or averaging across a basin in the absence of station data. Despite these differences stemming from the

305   challenges of using limited in-situ observations, the basin-aggregated phase diagrams appear reasonably representative ~~in~~ at capturing the broader hydroclimate conditions interpreted from phase trajectories.

4.6 ~~Towards Visualizing the Type and Extent of Snow Drought Across Space~~

~~We applied SNOTEL station data to create the phase diagrams, but a challenge in mountain environments is the lack of reliable, well-distributed~~

4.5.1 Basin-Averaged Phase Diagrams for an Observation-Limited Region

The Susquehanna River Basin of the northeastern U.S. includes both seasonal and ephemeral snowpacks (**?**; Figure 7a) that occur during extended winter (December-March; Figure 7b). Although snowpack in the Susquehanna Basin is not as critical for downstream water availability as in the western U.S., it supports winter recreation and is a critical component for ecosystems function in northern forests (**?**). The Susquehanna is highly susceptible to flooding, especially during snowmelt or rain-on-snow events that contribute to enhanced runoff (**?**). Even in locations without long-term ~~observations.In lieu of station data, gridded observational products commonly inform natural resource decision-making and research efforts.The necessary components exist to create phase diagrams using gridded meteorological products (??), observation-based snow datasets (??), and output from hydrological simulations (?). The challenge is how to aggregate spatial information to become meaningful in complex terrain. We have performed a first step towards this goal. Initial methods to broaden the approach could be performed by: (1) binning regions by similar elevation, watershed, slope, aspect, and /or land cover type; (2) identifying areas that co-vary together in time and space using techniques such as principal component or cluster analysis; and (3)subjective grouping based on anecdotal information from managers. Creating meaningful phase diagrams using spatially distributed information is the primary goal of our ongoing research. This will allow evaluation of snow drought in regions without long-term snow-observing networks such as in the northeastern~~ snowpack monitoring data, basin-averaged phase diagrams can be applied to highlight a range of drought outcomes. Four examples from the Susquehanna River Basin follow.

WY1988 demonstrates a dry winter ($< 25^{th}$ percentile precipitation) that oscillated between moderate (D1) snow drought and "Dry but Snowy" (up to 67th percentile SWE) conditions (Figure 7c). While WY1994 started off the winter season in moderate (D1) warm snow drought conditions, substantial improvement occurred from mid-December onward with consistently cold conditions and a wetter-than-average February (Figure 7d) bringing a near-record snowpack late spring snowpack (Figure 7b). The snowpack and saturated soils developed during the "Big Year" of WY1994 culminated in a large flood event in early April (**?**). A similar situation occurred in WY1996 (not shown) with extremely wet and snowy conditions leading up to a warm, windy, and wet January storm that coincided with saturated as well as frozen soils that contributed to overland flow and widespread flooding (**?**). WY1995 demonstrates another dry snow drought outcome, though with more severe snow drought conditions (as low as exceptional (D4)) but a slightly wetter overall winter than WY1988 (Figure 7e).

In 2016, a notable warm snow drought year occurred in the Northeastern U.S. ~~or other high mountain areas worldwide. Towards this end, we next provide examples of how spatially distributed products can visualize snow drought~~ with record temperatures (**?**) and closer-to-average winter precipitation leading to dry and warm snow drought (trajectories plotting to the right of the 1:1 line; Figure 7f). The exceptionally low snowfall (much of the winter ranged from D1 to D4) exacerbated drought conditions during the following drier-than-normal warm season, leading to 30%-70% crop losses (**?**). The Susquehanna

340 examples further indicate gridded products can be applied to create meaningful phase diagrams at the basin scale to track snow drought through time.

4.5.2 Snapshots from Water Year 2015 Across the Western U.S.

Using WY2015 as an example, gridded SWE and precipitation allow visualizing the spatial extent and type of snow drought across space. Peak warm snow drought conditions in the Pacific Northwest were occurring ~~in January~~ by 1 January 2015 (Figure

345 8a), consistent with the Paradise SNOTEL phase diagram (Figure 4b). ~~In January~~At this time, much of the Intermountain West and Rocky Mountain regions had near-average or above average (percentiles greater than the 50th, represented in purple), while several ranges in the southern tier of the wUS (e.g., California's Sierra Nevada, the southern Basin and Range, and the Uinta Mountains in Utah) were experiencing dry snow drought conditions. By ~~the~~ 1 February 2015 (Figure 8b) an expansion of areas experiencing dry snow drought occurred throughout the central and southern Rocky Mountains. Warm snow drought

350 had started to transition to dry snow drought in the Pacific Northwest. Dry conditions continued through February (Figure 8c). ~~By~~ On 1 April 2015, nearly all mountain regions were experiencing snow drought conditions (Figure 8d). Exceptions include the far northern Rockies, a few small areas in the Colorado Rockies, and the far northern Cascades.

The transition to dry snow drought in the Pacific Northwest (Figure 8d) was also observed at the Paradise SNOTEL (Figure 4b). While the hydrologic outcome of the early winter warm snow drought included earlier runoff timing resulting from more

355 frequent mid-winter runoff following rain-on-snow and rain instead of snow ((~~?~~)?; Figure 4c), the 1 April 2015 conditions indicate dry snow drought both spatially (Figure 8d) and at the station level (Figure 4b). This demonstrates the value of tracking snow drought and precipitation through time, as following the temporal evolution of hydroclimate allows outcomes (e.g., runoff and spatial patterns of snowpack anomalies) to be explained with more nuance. Such explanation is important as similar end-of-season SWE anomalies in space (compare Figures 4g, 4k, and 8d) ~~demonstrate markedly~~ show different hydrologic outcomes

360 (Figure 4c). Last, Figure 8e highlights an example of the differing elevational response of snow drought in the Sierra Nevada (percentiles increase with increasing elevation) and the Uinta Mountains (percentiles decrease with increasing elevation) for the same midwinter time. This example shows how sub-seasonal snowpack heterogeneity could create differing melt-season responses (i.e., earlier snow loss at lower elevations with increasing radiation and springtime warming) or ongoing avalanche hazards (i.e., higher elevation snowpacks are more prone to weakening when shallow).

365 ### 4.5.3 ~~Tracking Interannual Snow Drought Magnitude and Extent~~

~~The varying categories of snow drought and their spatial extent over large swaths of the wUS can be tracked through time (Figure ??). Sub-selecting snowpacks typically classified as seasonal in the wUS (?) using a median value of the snow seasonality metric (?) exceeding 0.5, three important time periods are examined. The first two times, 24 December (Figure~~

370 ~~??a) and 1 March, represents two important holiday periods when snow recreation-based tourism has an outsized impact on mountain economies (?). The third time, 1 April (Figure ??c), as well as 1 March (Figure ??b), represent important decision-making times for wUS water resources ?.~~

16

Time series of the percent of western United States seasonal snowpack area in various categories of snow drought (D0-D4) for: 24 December **(a)**, 1 March **(b)**, and 1 April **(c)**. The inset map at right shows the area (in blue) satisfying seasonal snowpacks over which the area calculation is performed.

In all cases, interannual variability ranges from less than 10% to more than 60% in December (Figure **??**a) and March (Figure **??**b). The maximum amount of area in snow drought on 1 April is less than 50%. The WY2015 snow drought stands out (Figure **??**b-c; see also Figure 6c-d), especially given the amount of area in the more severe snow drought categories (D2-D4). December and March snow droughts in the early 1990s appear to have undergone amelioration during March, as indicated by decreasing area.

Applying a Mann-Kendall test for trend (**?**) suggests 1 April and 24 December have experienced long-term increases in the amount of seasonal snowpacks in snow drought. The 1 April trend of 2.3% is more significant (p=0.00037) than the 3.3% trend for 24 December (p=0.06). The trend of 0.3 % for 1 March was not significant (p=0.87). These examples could be further extended to the mountain range or watershed scale of interest as well as subset by elevation. They could be extended to show percent of area in snow drought at the daily timescale to track conditions through a given year. In addition, these plots could be decomposed to show percent of area in warm or dry snow drought in order to track physical drivers of snow drought conditions.
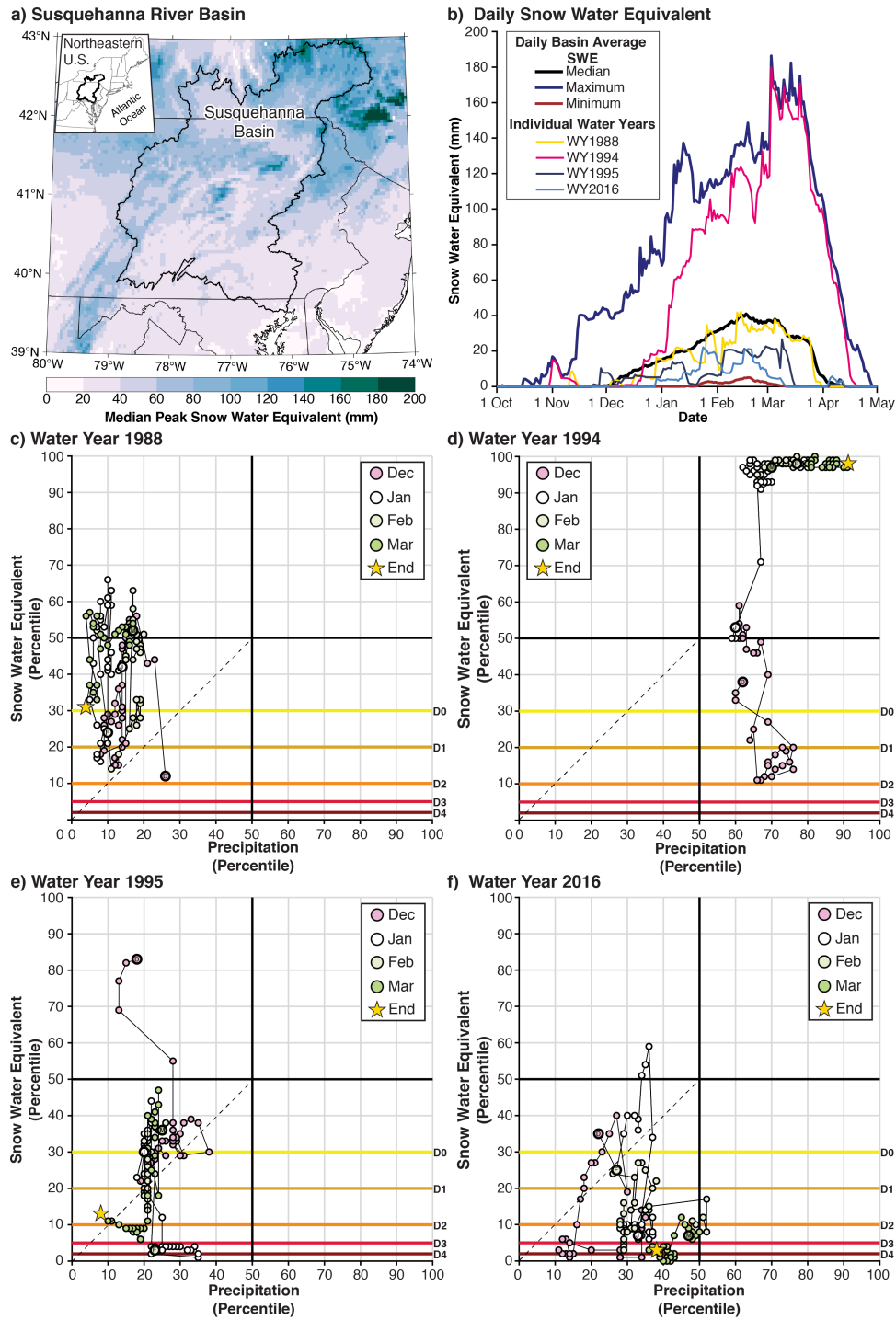
Figure 7. (a) Peak snow water equivalent (SWE) in the Susquehanna River Basin (b). Daily SWE climatology and time series of four water years. Phase diagrams for (c) Water Year (WY) 1988, (d) WY 1994, (e) WY 1995, and (f) WY 2016.
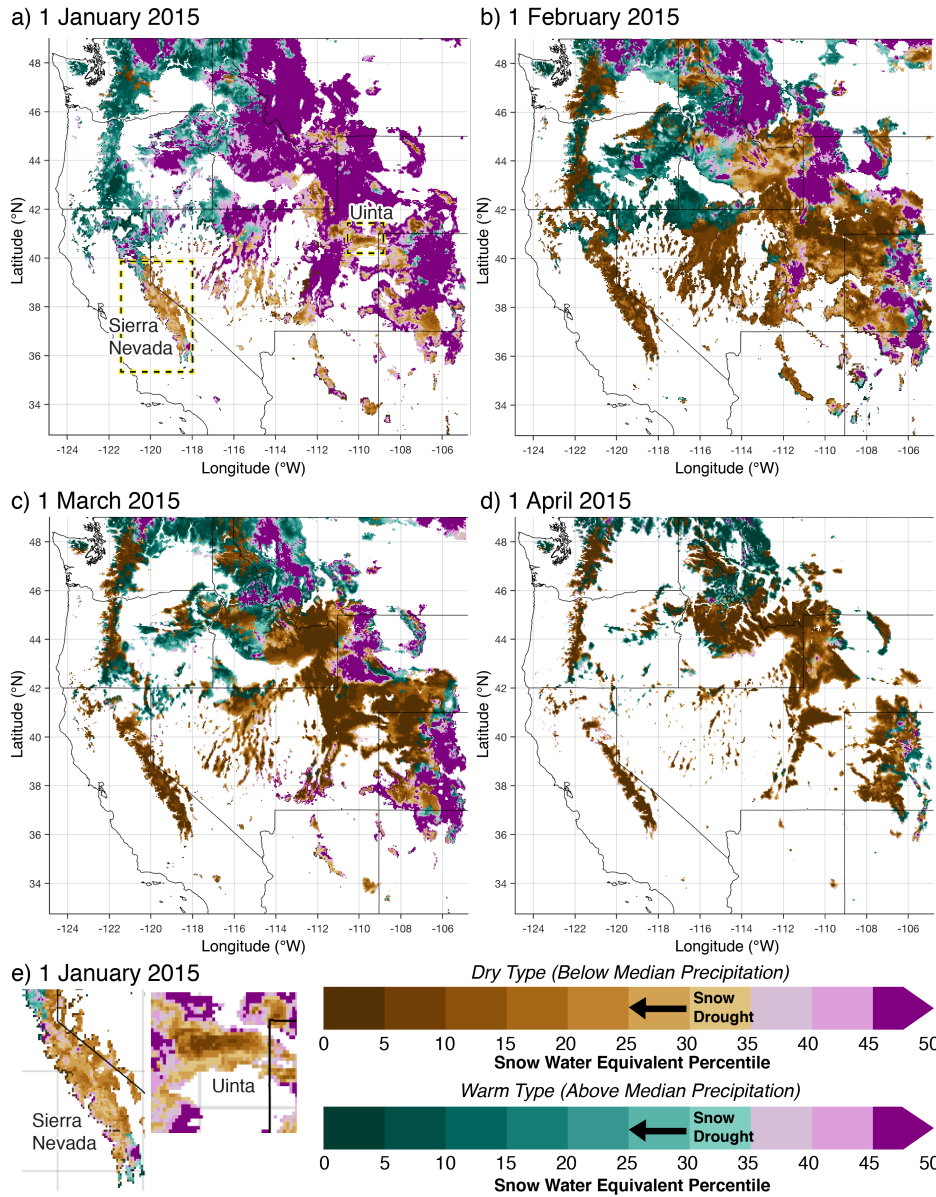
Figure 8. Spatial extent of snow drought conditions across the western United States on: **(a)** 1 January 2015, **(b)** 1 February 2015, **(c)** 1 March 2015, and **(d)** 1 April 2015. **(e)** The differing snow drought patterns across elevation in the Sierra Nevada (percentiles increase with increasing elevation) and the Uinta Mountains (percentiles decrease with increasing elevation). For clarity, only grid cells observing seasonal snowpacks (**?**) are shown.

4.6 Web-based Snow Drought Tracker Description

A snow drought tracker web application has been developed to provide users access to snow drought phase diagrams. The beta version is available at: https://wrcc.dri.edu/my/climate/snow-drought-tracker and simply requires users to set up a username/password to access it. The web tool is updated in near real-time across the wUS and Alaska. The SNOTEL network (**?**) is the backbone of the tool with over ~~700~~ 800 stations providing daily SWE, snow depth, precipitation, and temperature data. An interactive map (Figure 9a-b) allows for station selection via a graphical user interface. Once a station is selected, current year observations are displayed on the "Dashboard" by default (Figure 9c-d). As an example, the Mill-D North station in the Wasatch Mountains of northern Utah is shown (Figure 1b). The "Dashboard" will also display the most recent daily updated snow drought phase diagram (starting on October 1st of the WY2021; Figure 9e. The "Almanac" has several tabs showing daily SWE, snow depth, and precipitation absolute values, and percent of average SWE (Figure 9c). Note that because percent of average is more commonly used by managers, the first iteration of the tool uses percent of average (and the 80% threshold used by **?**) instead of percentiles and Drought Monitor thresholds as otherwise focused on in this manuscript. From the "Almanac" the month-to-date, calendar year-to-date, and WY-to-date precipitation values and percent of normal can be viewed (Figure 9d). In addition to the current year data found on the dashboard, historical data and graphics can be generated. Phase diagrams can be created for any year in the station record and daily time series plots can be generated for SWE, snow depth, precipitation, and temperature (e.g., Figure 9e). Figures ~~are available to download~~ can be downloaded as PNG or SVG files and historical data can be downloaded in CSV format. Beta testing of the snow drought tracker is being conducted by stakeholders including the National Weather Service, California Department of Water Resources, and state climatologists around the wUS. Other agencies will be encouraged to test the tool after the first round of testing and updates have concluded. Feedback from the testing will be incorporated into future upgrades of the snow drought tracker, with the goal of further developing a web-based product that ~~facilitates and~~ provides a science-to-service-to-practice interface (**?**). Some known limitations and gaps in the current version of the tool include the lack of spatial snow drought information (i.e., the river basin composites (~~Figure 6~~ Figures 6, 7), and 8 created using gridded products)~~or gridded data estimates (Figure 8~~) ~~)~~ and the need to incorporate elevation gradients into snow drought monitoring.
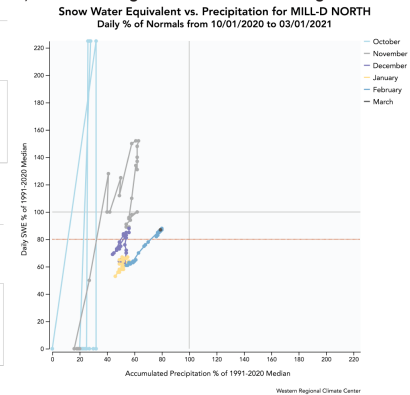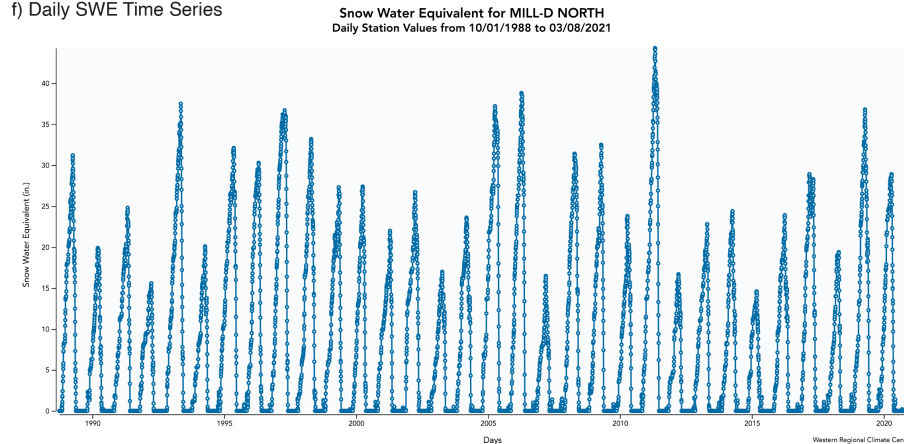
Figure 9. Screenshots from the beta Western Regional Climate Center (WRCC)'s Snow Drought Tracker. **(a)** Dashboard landing page. **(b)** Example screenshot assessing a station in a region of interest (inset). **(c)** Daily information tab from the Almanac. **(d)** Water-Year-to-Date Almanac tab. **(e)** Real-time phase diagram for water year 2021. **(f)** Daily snow water equivalent (SWE) time series for the period of record. Basemaps in **(a)** and **(b)** utilize ArcGIS® Online World Imagery by Esri. ArcGIS® is the intellectual property of Esri and are used herein under license. Copyright ©Esri. All rights reserved. For more information about Esri® software, please visit www.esri.com.

4.7 Limitations

4.7.1 Phase Diagrams

Our snow drought phase diagram visualization approach is not without limitations. ~~By~~ First, we used the full period of record available for stations to calculate percentiles. In cases where stations being compared have sufficient data (i.e., at least 20 years) but differing periods of record, selecting commonly overlapping periods from which to calculate percentiles may avoid biases created by a station whose full record captures anomalous conditions (e.g., a notable wet, dry, warm, or cold set of years) compared to a station with a shorter period of record. Second, by failing to include additional environmental controls on snowpack, such as temperature, radiation, and relative humidity, phase diagrams cannot tell a complete story of the drivers of snow accumulation, ablation, and/or melt. For example, the signal of a rain-on-snow event (**?**) was captured in the snow drought phase diagrams for Tahoe City Cross (see Figure 3) for an anomalously warm April AR (**?**). This event increased precipitation percentiles though SWE percentiles remained constant. However, when a rain-on-snow event increases net SWE, the phase diagram will not explicitly differentiate this from a snow accumulation event. Dry periods have differing snowpack outcomes during both the accumulation and ablation season depending on temperature (**??**) as well as how the snowpack energy budget is influenced by the deposition of dust or other light-absorbing particles on snow (**??**), cloud cover (**?**), and atmospheric moisture (**?**). How best to include these additional parameters that help to describes changes in the phase diagram trajectories is an area of future research. Collaborations with natural resource managers, practitioners, and decision makers will be instrumental in the development of locally- or regionally-specific snow drought thresholds. Ideally, such collaborations will facilitate the use of phase diagrams for monitoring efforts (at sub-seasonal-to-inter-annual scales) and be used to evaluate past hydroclimatic extremes to improve real-time water supply monitoring (**?**).

In addition to the development of locally-relevant thresholds, the identification of watershed-level sensitivity of streamflow to snow drought type and magnitude can add additional insight to drought monitoring, early warning, and how continued warming will influence mountain hydrology. Many western U.S. watersheds are characterized by dry summer conditions, relying upon snowmelt-derived groundwater recharge to maintain warm season streamflow (e.g., (**?**). However, exceptions occur in humid summer climates where snowpack plays a lesser role in controlling summer hydrologic regimes, i.e., summer flow is less dependent on peak SWE (**?**). This may be the case in lower elevation watersheds in the Pacific Northwest or in regions impacted by the North American Monsoon, a warm-season precipitation regime that **?** found augments low elevation evapotranspiration and high elevation streamflow. However, the 2016 snow drought in the Northeastern U.S. (Figure 7f) shows humid climates may experience water availability challenges with reduced snowpack compounding dry and hot conditions during the warm season (**?**). Watershed-specific hydroclimatic analyses could help identify and rank the risks snow drought poses to water availability and could help inform adaptation strategies to offset reductions in water availability from projected snowpack decline **?**.

4.7.2 Percentiles Versus Percent of Median: The Wilson Glade, UT avalanche incident

At present, phase diagrams on the WRCC Snow Drought Tracker show percent of median, rather than percentiles. Percent of median is ~~more~~ commonly used in snow drought communication by the National Integrated Drought Information System's Snow Drought Tracker website (https://www.drought.gov/topics/snow-drought). A difficulty with using a percent of average rather than a percentile-based approach is it does not reflect the distribution of conditions. Percentile-based approaches provide more direct information about a given date's conditions with respect to the range of previously experienced conditions. To highlight the value of a percentile-based approach and how phase diagrams can be employed to assess the evolution of snowpack stability, an example from a 2021 avalanche incident in the Wasatch Mountains is explored.

On 11 February 2021, a skier triggered failure of a deep persistent slab R4-D2.5 avalanche event (R4 implies a large runout relative to path size, D2.5 indicates sufficiently large to bury, injure, or kill a person; **?**) occurred on a northeast aspect at approximately 2900 m in the Wilson Glade region of the central Wasatch Mountains. Despite heroic rescue efforts, four fatalities resulted. A detailed report is available from the Utah Avalanche Center (UAC): https://utahavalanchecenter.org/avalanche/59084. The UAC's avalanche advisory for 11 February was high, indicating large human-triggered avalanches are very likely.

The phase diagram for the Mill-D North SNOTEL (Figure 10a; 3.3 km southeast of the accident site) shows early season November snowfall was followed by prolonged dry conditions into the winter months (downward and leftward trajectory), with D0 snow drought onset in early December (Figure 10a and (yellow arrow in Figure 10b)). Note snow drought onset occurs, perhaps non-intuitively, at approximately 85% of median snowpack. This indicates limited variability in SWE at this time and station: large deviations from the median value are relatively infrequent. The late November and early December dry spells led to snowpack accumulation falling behind the climatological average (Figure 10b). While some accumulation occurred during mid-December into early January, the rate of accumulation was less than climatology (Figure 10b), leading to a continued decline into D1 snow drought (Figure 10a). Percent of median SWE hovered around 65% leading up to the avalanche (Figure 10b), though SWE percentiles ~~fell into~~ approached the D2 category. A transition to ~~more active~~ stormier weather in late January into February followed with gains in SWE that mirrored climatology with little change in SWE percentile or percent of median (Figure 10b). The presence of a shallow snowpack during the dry, low radiation periods in November and December promoted the formation of a persistent weak layer with striated, 3-6 mm faceted grains buried 90 cm deep in the snowpack. According to the UAC, this is the layer where failure occurred on 11 February.

The snowpack conditions leading up to the Wilson Glade avalanche show the potential disconnect between percent of median and percentile. Prior to the loading events, the percent of median values (65%) between December and early February do not directly convey the infrequency of these values as percentiles can. Percentiles show that such conditions occurred only 10-20% of the time. The user's familiarity with a location will govern the meaningfulness of percent of medians through prior experience. On the other hand, percentiles provide perspective for less-familiar users to understand the ~~distribution and~~ state of the snowpack. Percentiles also allow comparisons between locations in terms of snow drought severity. By recognizing both as valuable, the option to view either on the snow drought tracker webtool is a planned improvement. Last, we recommend incorporation of percentiles into accident write-ups, such as provided by the UAC, to give this additional statistical perspective.
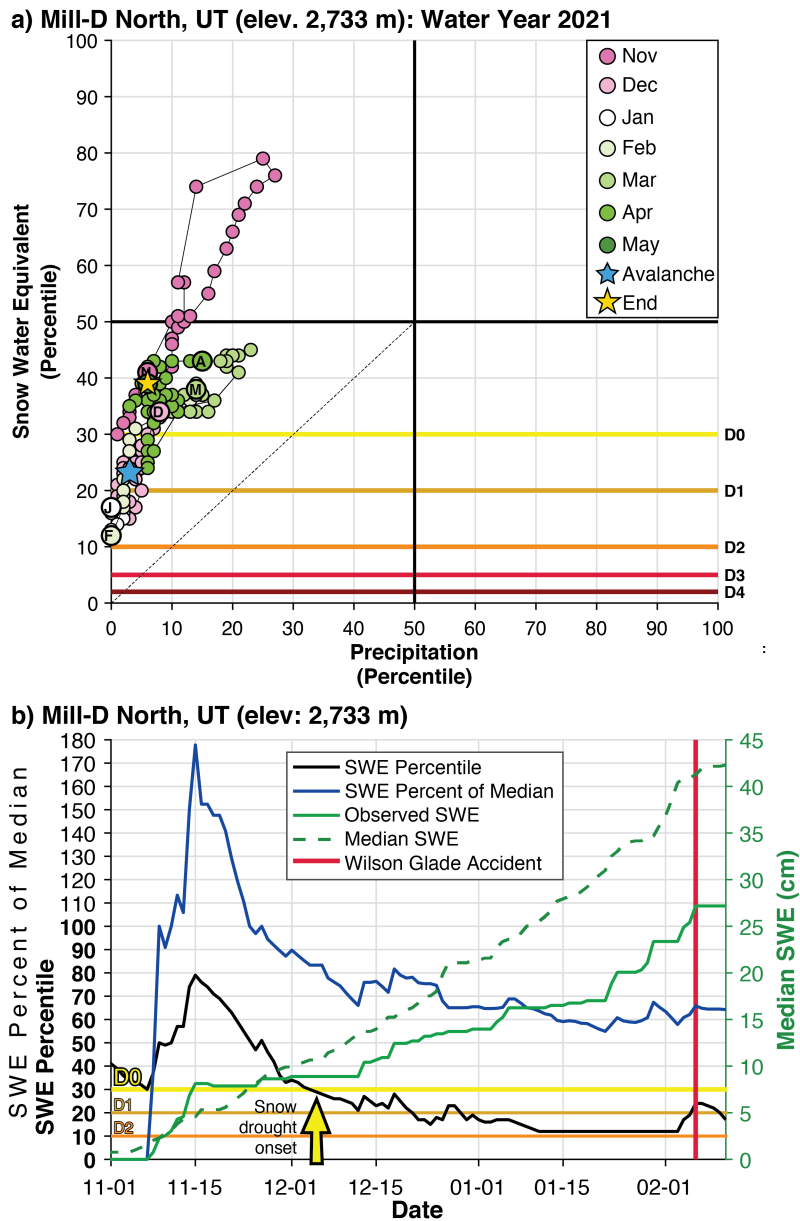
a) Mill-D North, UT (elev. 2,733 m): Water Year 2021

b) Mill-D North, UT (elev: 2,733 m)

Figure 10. (a) Phase diagram for Mill-D North SNOTEL in the Wasatch Mountains of Utah for WY2021. **(b)**. Time series of snow water equivalent (SWE) percentile (bold; left y-axis) and percent of median (left y-axis) and observed and median SWE (cm; dark blue and dashed green lines, respectively; right y-axis). The vertical red line shows the date of the Wilson Glade Avalanche accident. The horizontal gold line shows the percentile associated with ~~"Abnormally Dry" (D0)~~ the onset of snow drought conditions (D0).

5 Conclusions

Our primary goal was to demonstrate a visualization approach to show the temporal evolution of snow drought conditions, and more broadly mountain hydroclimatic conditions, through the cool season. When annotated, phase diagrams help "tell the story" of a snow season and can help communicate the weather and climate events that shaped the outcome of peak snowpack and lifecycle of the snowpack. We provided examples showing a range of applications in various snow climates for extreme years and how additional data such as spatially distributed SWE and precipitation as well as river discharge can further enhance the utility of information provided by phase diagrams. The spatial snow drought maps and basin-aggregated phase diagrams generated using gridded data products demonstrate an approach evaluating snow drought patterns across the landscape or in sparsely observed regions.

Our approach can be extended beyond addressing the noted limitations. While our primary purpose was to show the evolution of conditions in the current year, phase diagrams are easily produced for all previous years to allow comparisons of trajectories at seasonal or monthly timescales. These diagrams can incorporate forecasts of precipitation and SWE to show how snow drought conditions may evolve at subseasonal-to-seasonal timescales. For example, inclusion of bias corrected ensembles of medium range to subseasonal forecasts of precipitation and SWE from various forecasting center model(s) can create an ensemble of plausible trajectories (or cone of uncertainty) that would provide a probabilistic perspective to explore snow-drought evolution. They can also be applied to investigate how climate change may ~~permanently~~ alter phase diagram trajectories and/or residence times of WY snowpack conditions in particular quadrants of the phase diagram. However, as warming shifts the distribution of early, late, and spring peak snowpack towards lower values, it is worth considering holding the historic period from which percentiles are calculated constant over a management-relevant time period. This would reflect the historic conditions from which water management made assumptions about snowpack and water availability (**?**).

Ultimately, phase diagrams could become useful tools to provide climate services to both the public and decision-making audiences through early warning information on drought type, location, extent, and severity. The goal of these diagrams and the web-based tool is to alleviate some management concerns outlined in **?** and **?**, ~~namely~~ including runoff forecast timing errors, lack of upstream reservoir storage, and reductions in water supply reliability and water quality. These concerns can be start to be addressed through illuminating water supply uncertainties ~~and~~ across a range of hydroclimate conditions, enhancing the flexibility of subseasonal-to-seasonal water management practices, and improving coupled atmospheric and hydrologic forecast systems (**?**). By providing another means to communicate climate information, phase diagrams may help further develop the capacity to identify and to rapidly evaluate underlying vulnerabilities within and between human and natural systems that are susceptible to cascading and compounding effects (**??**). The Web-based tool producing the snow drought phase diagrams (https://wrcc-staging.dri.edu/my/climate/snow-drought-tracker) presented herein is concurrently being shared with groups responsible for communicating snowpack and mountain hydroclimate information to the public such as the U.S. National Weather Service as well as other water and natural resource managers. Last, snow drought phase diagrams can support innovative ways in thinking about how weather and hydroclimate variability influence the mountain environment. For example, phase diagrams help us re-frame snow drought as a time-dependent process rather than a point-in-time concept,

helping to contextualize hydrologic outcomes such as runoff efficiency. They also can be blended with other indicators relevant for ecosystem function (e.g., **?**) to explore how snow drought impacts forest health or limnnology as well as changing wildfire behavior (**?**). Our aim is for this information to aid mountain hydroclimate monitoring and drought early warning efforts, as well as promote scientific innovation in a changing mountain environment.